ORIGINAL PAPER

Arkady Neiman · Sergey Barsanov

Solid state interaction between V_2O_5 and MoO_3: specific features related to minor vanadia transfer

Abstract Vanadia transport, which is a minor reaction flux in the solid state reaction between V_2O_5 and MoO_3, was studied using chemical and neutron activation analyses and electron spectroscopy for chemical analysis. It was found that negligible quantities of vanadia were transferred in a molybdena briquette during the reaction. Vanadia was presumably localized in thin external layers of molybdena grains. The reaction potential difference U_r across a $Pt|MoO_3|V_2O_5|Pt$ cell was studied. It was shown that in this cell U_r was produced at the molybdena briquette and was due to vanadia transport. The U_r value changed with time in two stages. The reaction potential difference U_r was constant (or diminished slightly) at the first stage and dropped abruptly at the second stage. The duration of the first stage depended on the initial thickness of the MoO_3 briquette: the thicker the briquette, the longer the U_r value was nearly constant. Causes and probable mechanisms of U_r generation are discussed in different terms: chemical reaction, variation of a_{O_2} at the boundary between the reaction product and initialoxides, or surface spreading of the minor (V_2O_5 or $V_9Mo_6O_{40}$) diffusant. The last mechanism, which received the least study in the general case, was shown to be the most probable one for the reaction at hand.

Keywords Vanadium oxide · Molybdenum oxide · Electrical field effect · Composites · Flow potential

Introduction

The transport of polyvalent oxides (V_2O_5, MoO_3, WO_3) during solid state reactions is one of the most incom-

prehensible phenomena [1, 2, 3, 4]. To ascertain its mechanism, new experimental approaches need to be developed. One of them is the so-called electrochemical approach to solid phase reactions [1, 2, 3]. This approach includes (1) the study of the intrinsic electric potential self-generated in the cell:

$$AO_m|ABO_{m+n}|BO_n \qquad (1)$$

during the reaction, and (2) the analysis of the reaction rate as a function of the external potential applied to (or electric current passed through) cell 1.

In recent years these techniques were used to examine a number of solid state reactions involving MoO_3 (or WO_3) [1, 2, 3]. When an external electric field was applied, external polarization had an unexpectedly strong influence on the reaction rate and the reaction systems exhibited an apparent non-faradaic behavior. On the other hand, analysis of the internal electric field arising during the solid state interaction presents special interest.

To better understand specific features of the polyvalent metal transport, it is necessary to analyze as many reactions as possible, including mutual reactions between polyvalent oxides. The studies [5, 6] concerned with the solid state interaction between V_2O_5 and MoO_3 are noteworthy. This paper explores further the solid phase reaction between V_2O_5 and MoO_3. It is focused on the interaction under non-polarization conditions and examines the mechanism of this interaction, for which purpose the self-generated internal electric field was measured.

Phase equilibrium in the V_2O_5-MoO_3 system

In accordance with previous work [7, 8, 9], the solid solution of MoO_3 in V_2O_5 (α-phase) is formed at compositions close to V_2O_5. Molybdena solubility in V_2O_5 decreases from 25 to 10 mol% when the temperature drops from 640 to 500 °C [7, 8]. The nonstoichiometric chemical compound $V_{2-x}Mo_{1+x/2}O_{8-y}$ (β-phase; $0 \le x$

A. Neiman (✉) · S. Barsanov
Chemical Department, Ural State University,
620083 Ekaterinburg, Russia
E-mail: arkady.neiman@usu.ru
Tel.: +7-3432-617470
Fax: +7-3432-615978

≤ 0.3, $0 \le y \le 0.1$) is formed in the interval $1.5 \le [V]/[Mo] \le 2$ [7, 8]. Some of the vanadium atoms (several per cent) were found to be in the 4+ oxidation state in the α- and β-phases [9].

It was observed [9] that not more than 2% vanadia could dissolve in molybdena and form a solid solution under equilibrium conditions. However, our subsequent data show that the picture is not so simple: it seems more reasonable that the phase formed during penetration of V_2O_5 into the MoO_3 surface represents a two-part composite phase. The second part will be designated as "$^{V_2O_5}/MoO_3$" during the following discussion.

The oxides V_2O_5 and MoO_3, and also the phases in the V_2O_5-MoO_3 system, have structures like ReO_3, which may be described using a mixed coordination of polyvalent atoms (the coordination numbers being 4 or 6) [10].

Interaction between V_2O_5 and MoO_3

The solid state interaction between V_2O_5 and MoO_3 was studied by annealing diffusion pairs [5, 6]. The reaction products were localized both on V_2O_5 and MoO_3 briquettes (Fig. 1). The layer of reaction products on V_2O_5 was much thicker than on MoO_3. Briquettes of V_2O_5 gained mass and those of MoO_3 lost mass as a result of the interaction. These facts suggest that the reaction proceeded as a counter diffusion of V_2O_5 and MoO_3, where the flow of MoO_3 dominated. It was found that most of the V_2O_5 briquette was occupied by the solid solution of MoO_3 in V_2O_5 (α-phase). In accordance with the X-ray data, the product located at the initial interface between V_2O_5 and MoO_3 (Fig. 1) represented the $V_9Mo_6O_{40}$ compound (β-phase).
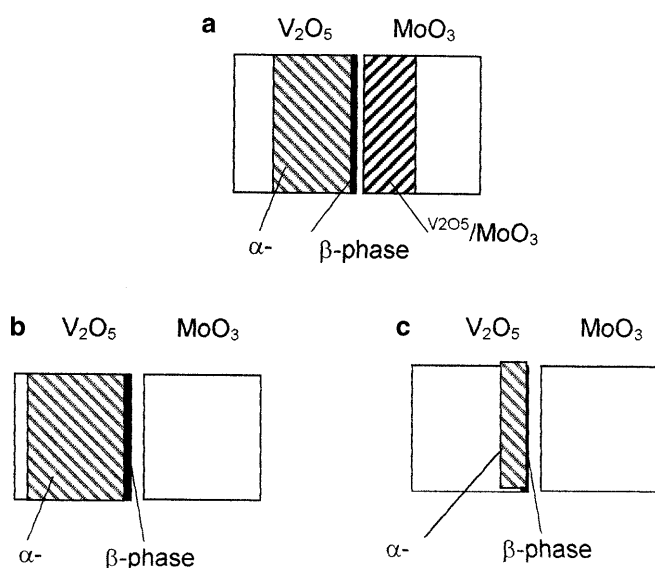

Fig. 1 Diagrams of the location of the products after solid state interaction between V_2O_5 and MoO_3: **a** anneals without external electric field applied; **b** anneals under (+)$MoO_3|V_2O_5$(−) external polarity; **c** anneals under (−)$MoO_3|V_2O_5$(+) external polarity

The product on the MoO_3 briquette differed in color from the MoO_3 substrate (grayish brown for the product and pale yellow for MoO_3). The X-ray diffraction and microprobe analyses did not reveal any other phases in addition to MoO_3 on the surface of the MoO_3 briquette. Owing to non-uniform coloration and spot-like location, the product will be assumed to be a composite of V_2O_5 or $V_9Mo_6O_{40}$ distributed onto the V_2O_5 surface "$^{V_2O_5}/MoO_3$". Thus, the model cell:

$$Pt|V_2O_5|MoO_3|Pt \qquad (2)$$

transformed to:

$$Pt|V_2O_5|\alpha|\beta|^{V_2O_5}/MoO_3|MoO_3|Pt \qquad (3)$$

during the reaction.

The reaction potential difference U_r had the following polarity at 600 °C [5, 6]:

$$(+)Pt|V_2O_5|MoO_3|Pt(-) \qquad (4)$$

The U_r value was about 100 mV during the initial hours of the interaction. It was found that U_r occurred at the MoO_3 briquette. When the temperature was decreased to 550 °C, U_r increased up to 130 mV. This type of temperature dependence is typical of so-called chemical cells. It has been proposed [5] that U_r self-generation in the cell 4 might be due to a process at the molybdena briquette, probably formation of the solid solution of V_2O_5 in MoO_3 rather than the appearance of α,β-phases.

Application of an external electric field to the cell 2 had consequences as described below. Firstly, the number of reaction products changed: the α,β-phases were located on the V_2O_5 briquette as before, but no product was formed on the MoO_3 briquette under the given conditions (Fig. 1c). Secondly, the synthesis rate of the α,β-phases expressed as $(l/V)_\tau$ increased for the polarity $(+)Pt|MoO_3|V_2O_5|Pt(-)$ and diminished for the opposite polarity (Fig. 2). The reaction was shown to be governed by diffusion under both polarization and non-polarization conditions [5].
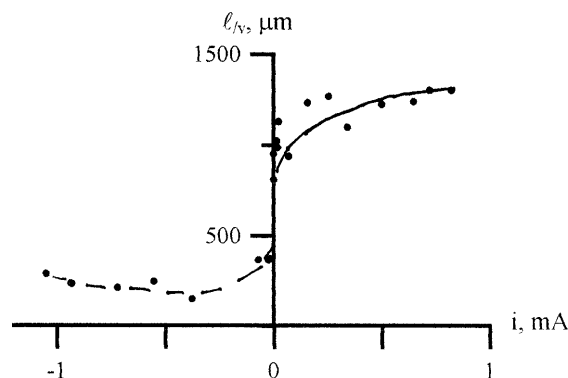

Fig. 2 Dependence of the product layer thickness on the V_2O_5 briquette upon the electric current (600 °C, 10 h)

Transport properties of phases in the V_2O_5-MoO_3 system

It is known from the literature [11, 12] that V_2O_5 is an electronic conductor. The nature of the conductivity of all phases in the V_2O_5-MoO_3 system was studied by the EMF method [5]. It was stated that the total conductivity (3–5 Ω^{-1} cm^{-1} at 600 °C) of the ceramics of the α- and β-phases was dominated by the electronic component (not less than 99%). The total conductivity of 2 mol% V_2O_5 and MoO_3 was lower ($\sigma_{V_2O_5/MoO_3} \approx 5 \times 10^{-5}$ Ω^{-1} cm^{-1} and $\sigma_{MoO_3} \approx 5 \times 10^{-6}$ Ω^{-1} cm^{-1} at 600 °C). However, they appeared to be mixed ionic-electronic conductors with the ionic component of the conductivity being not less than 55% at 600 °C.

The following conclusions can be drawn from an analysis of the literature data concerning the reaction kinetics, the phase equilibrium, and phase properties in the V_2O_5-MoO_3 system:

1. V_2O_5 and MoO_3 interact via counter-diffusion of V_2O_5 and MoO_3, where the molybdena flux dominates. Three products are formed. This is fundamentally different from numerical reactions involving MoO_3 [1, 2, 3], where only molybdena transport was observed.
2. Two products (α,β-phases) are electronic conductors located at the V_2O_5 briquette, where the electronic conductivity is also predominant. The third product, $^{V_2O_5}/MoO_3$ probably, is located at the MoO_3 briquette and is a mixed ionic-electronic conductor similar to MoO_3.
3. The interaction in the cell 2 is accompanied by self-generation of a relatively high U_r compared to the reaction involving MoO_3 [1, 2, 3]. The reaction potential difference occurs at the MoO_3 briquette (mixed ionic-electronic conductor) and is connected with the vanadia transfer being a minor reaction flux.
4. The cell 2 exhibits anomalous behavior in an external electric field. The growth rate of the α,β-phases (electronic conductors) strongly depends on the external polarization direction, while the $^{V_2O_5}/MoO_3$ composite (mixed ionic-electronic conductor) is not synthesized in an external field, at least visually, i.e. an external electric field inhibits V_2O_5 components onto the internal surface of MoO_3.

From what has been said above, it follows that the most interesting and unusual results concerning the kinetics of the solid state reaction between V_2O_5 and MoO_3 are due to the vanadia reaction flux being a minor reaction flux. Firstly, this flux causes self-generation of the reaction potential difference and, secondly, is retarded under the influence of an external electric field irrespective of its direction. The observed phenomena are very complex and incomprehensible and, therefore, it would be wise to analyze them in steps. Thus, the vanadia transfer in the absence of an external electric field will be considered in this work. Since this transport is connected with generation of the U_r signal, it is of special interest to establish any relations between the $^{V_2O_5}/MoO_3$ composite kinetics and the behavior of the reaction potential difference.

Experimental

Ceramic disks (10×1 mm) of V_2O_5 (ultrahigh purity) and MoO_3 (chemically pure) were prepared by pressing (1600 kg cm^{-2}) and subsequent sintering at 600 °C for 24 h. The sintered briquettes had a 30% porosity. The briquettes were ground with 10-μm abrasive paper, weighed, and clamped in reaction pairs. They were inserted in a holder between platinum electrodes (1×1 cm) and placed in a furnace heated to 600 °C beforehand. The annealed briquettes were separated and the disks were weighed to within ± 0.0001 g using commercial balances. Then the briquettes were broken perpendicular to the reaction surface and the thickness of the product layer was measured by an MBS-9 optical microscope.

The vanadia content of the MoO_3 reaction briquettes was determined by neutron activation analysis (NAA) and chemical analysis (CA) methods. A GC1518 detector measured the neutron-induced activity of the MoO_3 reaction briquettes. The chemical analysis of the vanadia content in the molybdena reaction briquettes involved potentiometric titration with preliminary separation of MoO_3.

The open-circuit reaction potential difference, which was spontaneously produced by the reaction couple 4, was measured by digital voltmeters whose input resistance was at least two orders of magnitude higher than that of the experimental cell. If a complex model cell of more than two briquettes was used, a thin platinum powder was fired on both sides of the briquettes to provide a reliable electric contact. To eliminate stray electric fields, the experimental cell was surrounded by a grounded shield.

The temperature was maintained by a VRT-3 unit with an accuracy of ± 1 K. X-ray patterns were registered using a DRF-2.0 diffractometer in Cu K_α radiation. The method of electron spectroscopy for chemical analysis (ESCA) was realized in a VG ESCA LAB HP device.

$V_9Mo_6O_{40}$ and $^{V_2O_5}/MoO_3$ compounds were synthesized from individual V_2O_5 and MoO_3 by a standard ceramic technique when the powder mixture of an assigned composition was annealed repeatedly and the temperature was increased in steps (Table 1). The annealed compounds were combined with intermediate grinding in a mortar from technical jasper. The phase composition was determined using X-ray analysis (DRF-2.0 apparatus).

Table 1 The conditions for $V_9Mo_6O_{40}$ and $^{V_2O_5}/MoO_3$ sample preparation

Powder mixture composition	Annealing conditions		
	First anneal	Second anneal	Third anneal
$V_9Mo_6O_{40}$ (43 mol% V_2O_5-57 mol% MoO_3)	5 h, 500 °C	10 h, 550 °C	75 h, 600 °C
$^{V_2O_5}/MoO_3$ (2 mol% V_2O_5-98 mol% MoO_3)	5 h, 500 °C	10 h, 550 °C	25 h, 600 °C

Results

Experimental evidence for vanadia transport
in the solid state reaction between V_2O_5 and MoO_3

The main difficulty encountered in earlier work [5, 6] was
the impossibility to determine how much vanadia was
transferred into a MoO_3 briquette. The basic experi-
mental parameter of the process rate (changes in the
mass of V_2O_5 or MoO_3 briquettes) was determined by
the predominant molybdena flux. The thickness of the
phase formed on the MoO_3 surface and visible in a
microscope cannot be directly related to the diffused
quantity of vanadia. It does not give any idea about
the mode or the density of V_2O_5 distribution inside the
MoO_3 substrate. Therefore the vanadia content of the
reaction MoO_3 briquettes was measured by independent
methods of CA, NAA, and ESCA. Values obtained by
the CA and NAA methods are given in Table 2. The
average flux density ($J_{V_2O_5}$) was calculated from the re-
lation:

$$J_{V_2O_5} = m^*_{V_2O_5}/(\tau S) \tag{5}$$

where, $m^*_{V_2O_5}$ is the mass of vanadia diffused inside the
MoO_3 briquette as determined by CA and NAA meth-
ods, τ is the annealing time, and S is the contact area of
the briquettes. One can see that average values of the
mass of diffused vanadia (and average vanadia flux
densities) detected by these independent methods differ
by 20% or less. Therefore it may be assumed that values
obtained by these methods are in satisfactory agreement.
When the briquettes were annealed at 600 °C for 10 h, a
relatively small quantity of V_2O_5 ($\sim 4 \times 10^{-4}$ g) was
transported inside the MoO_3 briquette. This corresponds
to the average flux density of 1.45×10^{-8} g s^{-1} cm^{-2}. Since
reaction fluxes (V_2O_5 and MoO_3) are opposite, the
molybdena average flux density may be calculated as:

$$J_{MoO_3} = (\Delta m_{V_2O_5} + m^*_{V_2O_5})/(\tau S) \tag{6}$$

where $\Delta m_{V_2O_5}$ is the average change in the mass of the
V_2O_5 briquette after the interaction. Given similar con-
ditions, the MoO_3 average flux was one order of mag-
nitude larger and was equal to 1.3×10^{-7} g s^{-1} cm^{-2}.

The available data suggest that vanadia transport
indeed occurred in this reaction and diffused quantities
of V_2O_5 were large enough. However, all these findings
do not allow establishing the actual state (solid solution
or individual compound) and the V_2O_5 diffusant distri-
bution (surface, volume, or mixed) in the MoO_3
briquette. Visually, the MoO_3 reaction briquette changes
in color from pale yellow to grayish brown, but this may

be due to diffusion and localization of vanadia in thin
external layers of MoO_3 grains (microheterogeinity is
supposed). We noted that the color of the layer on MoO_3
faded to pale yellow (the color of MoO_3) after the sample
was stored at room temperature in air for two days.

We examined MoO_3 reaction briquettes by ESCA in
addition to CA and NAA to ascertain vanadia pene-
tration into the MoO_3 briquette. Several experiments
were carried out: the molybdena surface in contact with
(1) a V_2O_5 briquette and (2) a platinum plate. The ratio
[V]/[Mo] was found to be 0.24 on the surface (1).
However, this value may be overestimated since several
visually discernible β-phase crystals remained on the
surface after separation of the briquettes. After the ex-
ternal layer (50 μm) was removed, repeated analysis did
not reveal any vanadia. Moreover, vanadia was not
detected on the surface (2). This may be due to the
following reasons:

1. ESCA was insufficiently sensitivite to the vanadia
   quantities distributed on the surface of the MoO_3
   grains.
2. At elevated temperatures the V_2O_5-enriched layer
   (V_2O_5/MoO_3 composite) is located on MoO_3 grains,
   but vanadia can diffuse into the depth on cooling (or,
   otherwise, MoO_3 can out-diffuse and enrich the sur-
   face on cooling). It is worth noting that the ESCA
   analysis was carried out several days after annealing
   and the above process could take place during that
   period. These speculations seem to be the most
   plausible explanation of the ESCA data for the
   MoO_3 briquette.

It is noteworthy that the valence of Mo atoms in all
the samples analyzed by ESCA was equal to 6, i.e.
molybdena was not partially reduced during the
reaction.

Reaction potential difference during interaction
between V_2O_5 and MoO_3

We write the polarity of U_r in the cell 2 again:

$$(-)Pt|MoO_3|V_2O_5|Pt(+) \tag{7}$$

The analysis of the reaction potential difference showed
that the time dependence of U_r had two main clearly
pronounced regions (Fig. 3). The potential difference U_r
was constant or decreased slightly from 100 to 70 mV
during the initial hours of interaction, and then dropped
sharply. In this connectizon, many questions arise
concerning the origin, distribution, and time behavior
of U_r.

Table 2 Mass of vanadia dif-
fused into MoO_3 pellet and
average flux density

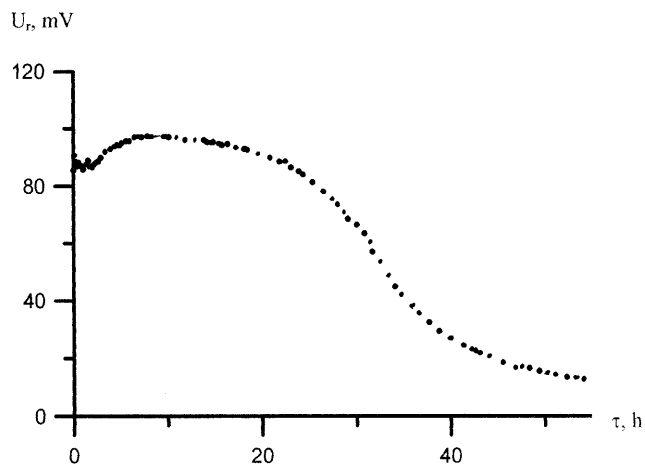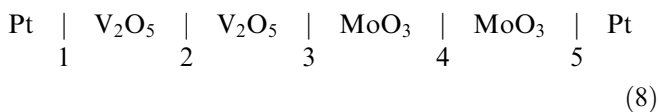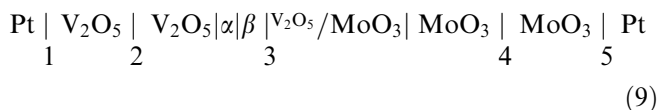| Type of analysis	Chemical analysis	Neutron activation analysis	Average value
Mass of vanadia diffused (g)	3.5×10^{-4}	4.7×10^{-4}	$(4.1 \pm 0.6) \times 10^{-4}$
Average flux density (g s^{-1} cm^{-2})	1.2×10^{-8}	1.7×10^{-8}	$(1.45 \pm 0.25) \times 10^{-8}$

U_r, mV

Fig. 3 Character of the time dependence of the reaction potential difference in the model cell 4

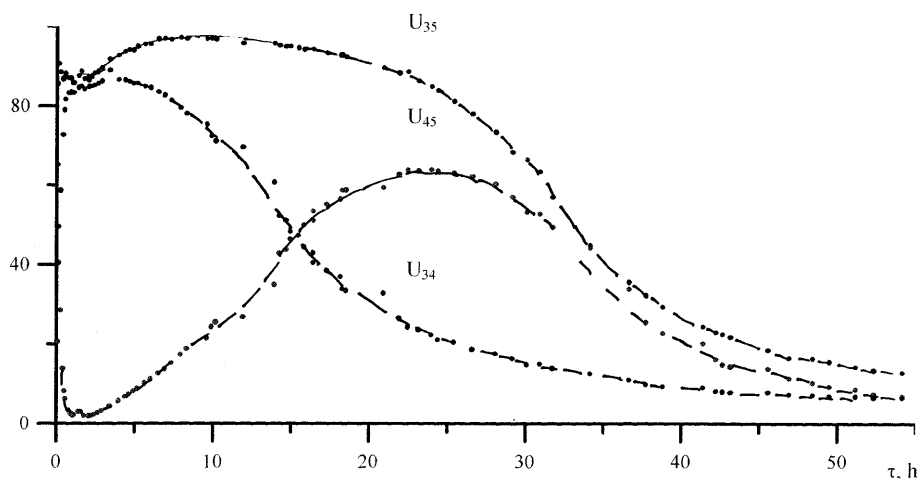The U_r distribution in different parts of the reaction cell 4 was determined using the following model cell:

$$\text{Pt} \mid \underset{1}{\text{V}_2\text{O}_5} \mid \underset{2}{\text{V}_2\text{O}_5} \mid \underset{3}{\text{MoO}_3} \mid \underset{4}{\text{MoO}_3} \mid \underset{5}{\text{Pt}} \tag{8}$$

Electrodes from a fine Pt powder were fired beforehand on both sides of each briquette and very thin Pt wires were inserted at boundaries 2, 3 and 4 during the cell assembly. During subsequent interaction, the cell transformed as:

$$\text{Pt} \mid \underset{1}{\text{V}_2\text{O}_5} \mid \underset{2}{\text{V}_2\text{O}_5|\alpha|\beta} \mid^{\text{V}_2\text{O}_5}/\text{MoO}_3| \underset{4}{\text{MoO}_3} \mid \underset{}{\text{MoO}_3} \mid \underset{5}{\text{Pt}} \tag{9}$$

Reliable data concerning the location of U_r in situ were obtained from measurements of internal voltages between the briquettes (U_{15}, U_{12}, U_{23}, U_{34}, U_{45}) (Fig. 4). The voltage U_{35} was nearly constant (100 ± 10 mV), while U_{45} increased monotonically and U_{34} diminished (Fig. 4). The values of U_{12} and U_{23} did not exceed 1 mV.
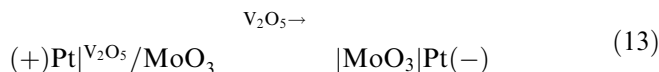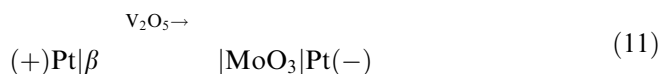
Therefore self-generation of U_r was related to the process at MoO_3 rather than the V_2O_5 briquette (MoO_3 [13] and the MoO_3-based phase [5] are mixed ionic-electronic conductors and ionic conductivity is connected probably with O^{2-} ions, whereas V_2O_5, α- and β-phases are electronic conductors in similar conditions) (Fig. 4).

When U_r of the cell 4 was measured during a longer period of time, the following unusual result was obtained: the region of constant (or slightly diminishing) U_r depended on the initial thickness of the MoO_3 briquette, that is, the thicker the briquette, the longer the region of nearly constant U_r (Fig. 5). Additional experiments were performed to explain this unusual behavior. First, we took into account the complexity of the $\beta|MoO_3$ boundary where U_r self-generation occurred:

$$\begin{array}{ll} \text{V}_2\text{O}_5 \rightarrow & \\ \beta & |^{\text{V}_2\text{O}_5}/\text{MoO}_3|\text{MoO}_3 \end{array} \tag{10}$$

We studied the following model cells that are parts of cell 10:

$$\begin{array}{ll} & \text{V}_2\text{O}_5\rightarrow \\ (+)\text{Pt}|\beta & |\text{MoO}_3|\text{Pt}(-) \end{array} \tag{11}$$

$$(+)\text{Pt}|\beta|^{\text{V}_2\text{O}_5}/\text{MoO}_3|\text{Pt}(-) \tag{12}$$

$$\begin{array}{ll} & \text{V}_2\text{O}_5\rightarrow \\ (+)\text{Pt}|^{\text{V}_2\text{O}_5}/\text{MoO}_3 & |\text{MoO}_3|\text{Pt}(-) \end{array} \tag{13}$$

The initial composition of the β-phase corresponded to $V_9Mo_6O_{40}$. The vanadia concentration of $^{V_2O_5}/MoO_3$ was equal to 2 mol% V_2O_5.

To understand processes in the cells 11, 12, 13, one should consider the distribution of the vanadia chemical potential ($\mu_{V_2O_5}$) in cell 3. As can be seen from Fig. 6, cell 11 is more complex than cells 12 and 13. The process that determines the potential in cell 11 is formation of $^{V_2O_5}/MoO_3$, while the probable process in cell 13 is redistribution of V_2O_5 or MoO_3 between MoO_3 and $^{V_2O_5}/MoO_3$. Since $\mu_{V_2O_5}$ (μ_{MoO_3}) is similar for both phases in cell 12, the β-phase ($V_9Mo_6O_{40}$) and

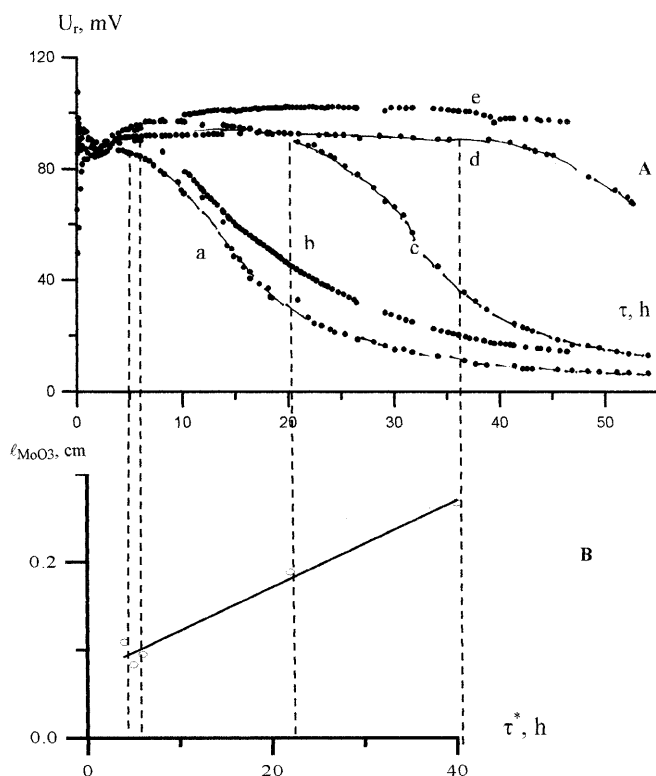**Fig. 4** Time dependencies of U_r upon the parts of cell 8 (600 °C)

Fig. 5 A Time dependencies of U_r in cell 4 with different thicknesses of molybdena pellet (600 °C): *a* 0.83 mm, *b* 0.95 mm, *c* 1.90 mm, *d* 2.72 mm, *e* 3.5 mm. **B** Duration of period with approximately constant U_r in cell 1 (τ^*) from the thicknesses of the initial MoO_3 briquettes (*l*)
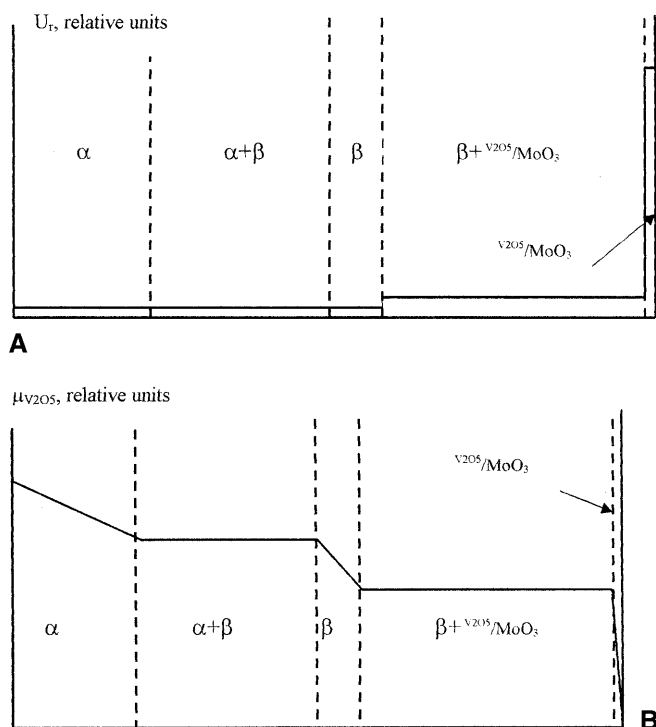

Fig. 6 A Distribution of reaction potential difference on the parts of cell 3. **B** Distribution of vanadia chemical potential upon the phases in the V_2O_5-MoO_3 system

V_2O_5/MoO_3 are saturated with vanadia and molybdena, respectively.

To find out whether a mass transfer occurred, the reaction surfaces of the briquettes were examined visually and in an optical microscope after contact annealing. No changes were observed for cell 12, a fact which probably points to the absence of mass transport. On the other hand, the color of the MoO_3 briquettes changed owing to V_2O_5 penetration. The vanadia transport direction and polarity are shown in cells 11, 12, 13. It was found that U_r was more positive at the briquette with a larger vanadia content. The evolution of U_r with time is shown in Fig. 6c and Fig. 7. One can see that the time dependence of U_r in cells 11 and 13, where V_2O_5/MoO_3 is formed, is similar to that in the cell 4. However, U_r in cell 12, where V_2O_5/MoO_3 was already formed and saturated with V_2O_5, was only 1–3 mV (Fig. 5). Thus, it may be stated that the total U_r of the V_2O_5-MoO_3 interaction is produced in the zone of the composite formation and homogenization at MoO_3, i.e. at the boundary between V_2O_5/MoO_3 and MoO_3, which moves deeper into MoO_3 during the reaction.

Discussion

The mechanism of V_2O_5 and MoO_3 interaction and the reaction transport present a special interest for a number of reasons:

1. V_2O_5 and MoO_3 have similar structures [10].

(12) (+)Pt | β | MoO_3 | Pt(-)

(13) (+)Pt | β | V_2O_5/MoO_3 $V_2O_5\rightarrow$ | Pt(-)

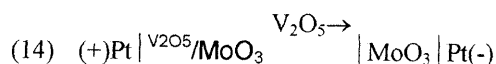(14) (+)Pt | V_2O_5/MoO_3 $V_2O_5\rightarrow$ | MoO_3 | Pt(-)
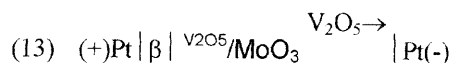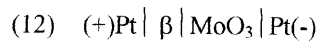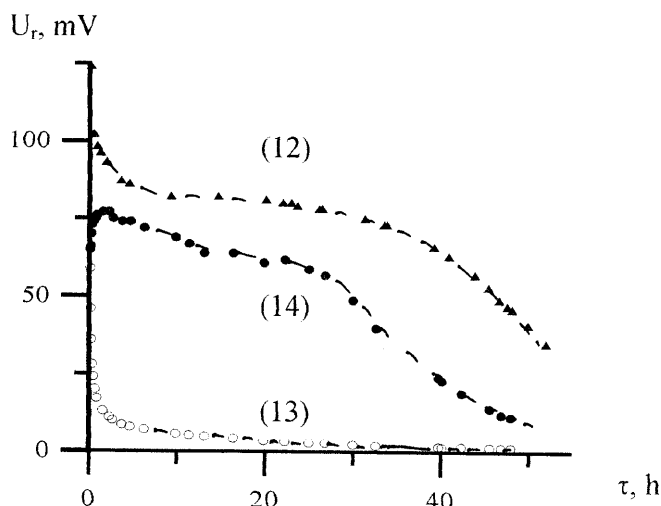
Fig. 7 Time dependencies of the reaction potential difference in the cells 11, 12, 13 (600 °C)

2. Both oxides belong to a class of substances whose specific surface energy is relatively low ($\alpha_{V_2O_5} = 9\times10^{-6}$ J s^{-1} m^{-2}, $\alpha_{MoO_3} = 6.5\times10^{-6}$ J s^{-1} m^{-2}) [14].
3. The electric conductivities of V_2O_5 and MoO_3 differ by five orders of magnitude; the nature of conductivity is also extremely different.
4. Mixed (V-O-Mo) transition diffusion states are possible.

The last point is beyond the scope of this paper and will be discussed elsewhere.

CAA and NAA experiments proved that vanadia diffused into MoO_3 against the background of a stronger (one order of magnitude) molybdena flux. However, only the minor vanadia flux led to self-generation of a strong U_r signal. The discussion below will deal with the origin, probable mechanisms of formation, the time evolution, and the dependence of the reaction potential difference on the MoO_3 substrate thickness in cell 4.

The origin and probable mechanisms of U_r formation

Theoretical and experimental background

The problem of the origin of U_r has been considered previously [1, 2, 3]. In accordance with [3], the following expression can be derived for U_r:

$$U_r = \left(\frac{z_B}{z_A}t_A - t_B\right)\frac{\Delta G^0}{z_i F} + \frac{1 - t_e}{4F}RT\ln\frac{a_{O_2}^1}{a_{O_2}^0} + U_{flow} \quad (14)$$

or:

$$U_r = U_r^1 + U_r^2 + U_r^3 \quad (15)$$

where ΔG° has the same meaning as for cell 2; z_k and t_k denote the charge and the transport number of the k species. The U_r value is determined by superposition of three terms associated with three possible processes:

1. Chemical interaction limited by the diffusion stage (U_r^1).
2. Variation of a_{O2} at reaction boundaries (U_r^2).
3. Diffusant spreading over the inner surface of a porous substrate (U_r^3).

Let us analyze each term in Eqs. 14 and 15. Firstly, In accordance with the equations:

$$U_r^1 = \left(\frac{z_B}{z_A}t_A - t_B\right)\frac{\Delta G^0}{z_i F} \quad (16)$$

The U_r polarity is determined by the direction of cation diffusion. The U_r value depends on the cation charge and transport number, and variation of the Gibbs free energy as a result of interaction. Thus, U_r^1 depends on the transport properties of the reaction product and is independent of the properties of the initial reactants. Since gaseous spaces in cells 1 and 2 are not separated, then for O^{2-} ionic conductivity:

$$t_{O2-} \gg t_{Az+}, B_{y+} \quad (17)$$

and:

$$U_r^1 \equiv 0 \quad (18)$$

This conclusion is supported by the data reported in [3]. On the other hand, in the case of cation conductors (Na-β-Al$_2$O$_3$, LiNbO$_3$), U_r obeys Eq. 16 and does not depend on time [3]. Obviously, U_r should be equal to zero if the synthesized products have predominantly electron conductivity ($t_e = 1$). It is easy to see that in this case:

$$t_e \gg t_{Az+, By+} \quad (19)$$

Experimentally measured U_r was nearly zero [3] when such electronic conductors as NiFe$_2$O$_4$ and PbZrO$_3$ were synthesized from oxides.

Secondly, the term:

$$U_r^2 = \frac{1 - t_e}{4F}RT\ln\frac{a_{O_2}'}{a_{O_2}''} \quad (20)$$

is determined by the difference of gaseous oxygen activities at product|oxide ($a_{O_2}^1 \cdot a_{O_2}^0$) boundaries and depends on the ionic part of the total conductivity. This term is mostsignificant for chemical reactions, which are accompanied by redox processes at reaction boundaries. In this case, every boundary becomes a getter with a constant a_{O2} at a given temperature [12]. The term U_r^2 is often uncertain since it depends on the gaseous permeability of "initial oxide/product" boundaries. If the permeability is high, a_{O2} will equalize at different boundaries of cell 2 and, consequently, the experimentally measured value of U_r^2 will decrease.

Finally, the third term is due to diffusant heterophase dispersion and spreading on the inner surface of a porous substrate:

$$U_r^3 = U_{flow} \quad (21)$$

This term is the most incomprehensible and unusual for solid phase systems. It appears owing to the recently discovered phenomenon of solid state spreading. This process is observed in the systems V_2O_5-TiO_2, MoO_3-TiO_2 [14, 15, 16], MoO_3-$PbMoO_4$, WO_3-$CdWO_4$, WO_3-$ZnWO_4$, MoO_3-Al_2O_3 [17], and WO_3-$CaWO_4$ [18], where MoO_3, V_2O_5, and WO_3 spread over the substrate surface. Another example of solid state dispersion and spreading is the behavior of Ga_2O_3 and In_2O_3 ceramics or coarse-grain powders in contact with α-Al_2O_3 single-crystal supports [20]. All experimental temperatures were much lower than any liquid phase temperature. Consequently, the diffusant would be transferred as a solid in the form of a "quasi-liquid".

The microscopic mechanism of solid state spreading remains unknown. However, a negative change of the free energy, ΔF, should take place at the macroscopic level [14], i.e.:

$$\Delta F = \alpha_d \Delta S_d - \alpha_s \Delta S_s - \alpha_{d/s} \Delta S_{d/s} < 0 \qquad (22)$$

where α_d and α_s denote the specific surface free energy of the diffusant and the substrate, respectively; $\alpha_{d/s}$ is the specific free energy of the interface between the diffusant and the substrate; ΔS_d, ΔS_s, and $\Delta S_{d/s}$ stand for the surface area of the diffusant, the substrate, and the interface between these two, respectively.

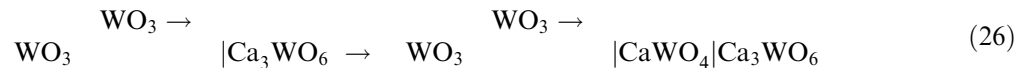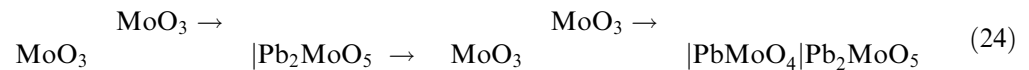Solid state spreading has been found [17] to proceed in several stages. Wetting of the surface of $PbMoO_4$, $CdWO_4$, $ZnWO_4$, and Al_2O_3 single crystals by MoO_3 and WO_3 was observed [17]. Those stages are as follows:

1. Adsorption of diffusant grains onto the substrate surface.
2. Smoothing of the diffusant grains, which become transparent and acquire a regular shape.
3. "Stretching" of transparent diffusant grains on the substrate surface and formation of islet films. The islet films preserve a regular shape.

said oxides were arranged quite oppositely with respect to their transport ability. This contradiction is evidence that solid state spreading is extremely sensitive to a number of external and internalparameters (mainly surface mobility).

Thus, the fact of solid spreading has been reliably established for a variety of systems with MoO_3, V_2O_5, and WO_3. Since spreading essentially is an interface process, there are no logical objections to its study and consideration in terms of classical colloid chemistry. The only principal difference is that spreading of a liquid over a solid surface is usually considered. In our case we obviously deal with the spreading of solids over the surface of another solid.

It is well known that when a liquid spreads over a substrate surface, a potential difference (flow potential) can appear. This potential is also possible for solid state spreading. The hypothesis of the flow potential produced in solid phase systems was advanced [3] to account for unusual values of the reaction potential difference in the following cells:

$$MoO_3 \qquad \begin{array}{c} MoO_3 \rightarrow \\ |Pb_2MoO_5 \rightarrow \quad MoO_3 \end{array} \qquad \begin{array}{c} MoO_3 \rightarrow \\ |PbMoO_4|Pb_2MoO_5 \end{array} \qquad (24)$$

$$MoO_3 \qquad \begin{array}{c} MoO_3 \rightarrow \\ |CdO \rightarrow \quad MoO_3 \end{array} \qquad \begin{array}{c} MoO_3 \rightarrow \\ |CdMoO_4|CdO \end{array} \qquad (25)$$

$$WO_3 \qquad \begin{array}{c} WO_3 \rightarrow \\ |Ca_3WO_6 \rightarrow \quad WO_3 \end{array} \qquad \begin{array}{c} WO_3 \rightarrow \\ |CaWO_4|Ca_3WO_6 \end{array} \qquad (26)$$

4. Merging of separate islets; the whole surface of the substrate is covered with a transparent film (≤ 0.1 μm thick) of the diffusant. Adsorption and solid state spreading continue and the thickness of the diffusant film increases. For example, the thickness of In_2O_3 film on α-Al_2O_3 single-crystal supports reaches 100 μm [19].
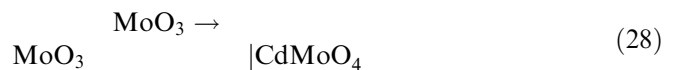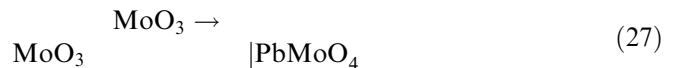
From the above discussion it follows that solid state spreading is characteristic of some oxides, namely MoO_3, V_2O_5, and WO_3. Researchers have examined the proneness of these oxides to spreading [14]. They compared the structures of V_2O_5 and MoO_3 and noted that the vanadia structure was more prone to cleavage than the molybdena structure. As a result, layer packages acquired some mobility, particularly in the case of V_2O_5 and, perhaps, MoO_3. The spreading would then be described as an exfoliation process. The tendency of oxides towards spreading was predicted [14] as:

$$V_2O_5 > MoO_3 > WO_3 \qquad (23)$$

On the other hand, considering the results of self- and reaction-diffusion studies, the author [4] stated that the

The reaction products ($PbMoO_4$, $CdMoO_4$, and $CaWO_4$) have mixed conductivity (O^{2-}, e^-, h), which leads to $U_r \approx 0$ estimated from Eq. 14. However, experimental U_r values were other than zero and were equal to 10–100 mV.

It was found [3] that in partial cells of the "diffusant product" type:

$$MoO_3 \qquad \begin{array}{c} MoO_3 \rightarrow \\ |PbMoO_4 \end{array} \qquad (27)$$

$$MoO_3 \qquad \begin{array}{c} MoO_3 \rightarrow \\ |CdMoO_4 \end{array} \qquad (28)$$

$$WO_3 \qquad \begin{array}{c} WO_3 \rightarrow \\ |CaWO_4 \end{array} \qquad (29)$$

where chemical interaction is impossible, the U_r polarity coincided with the polarity of cells 24, 25, 26 and corresponded to the positive potential at the diffusant briquette [3]:

$$(-) \text{ substrate|diffusant } (+) \qquad (30)$$

In addition, absolute values of U_r are similar for cells 24 and 27, cells 25 and 28, and cells 26 and 29. The ESCA analysis showed [3] that the surface of $PbMoO_4$ in cell 27, $CdMoO_4$ in cell 28, and $CaWO_4$ in cell 29 was largely enriched with MoO_3 and WO_3 after the experiments. On the strength of these findings it was inferred [3] that:

1. Solid state spreading and dispersion of the diffusant (MoO_3, WO_3) takes place on the surface of substrate grains ($PbMoO_4$, $CdMoO_4$, $CaWO_4$). Such spontaneous spreading is due to a high surface mobility and a low surface energy of MoO_3 and WO_3.
2. MoO_3 and WO_3 spread on the charged inner surface of ceramic substrates of molybdates and tungstates. The surface charge is "carried over" during spreading and, as a result, a potential difference is produced (Quincke effect).

Reaction between V_2O_5 and MoO_3

Let us analyze possible causes of U_r generation during the interaction between V_2O_5 and MoO_3 in line with the aforementioned arguments. Firstly, one can suppose that U_r is due to the charge separation in a thin reaction zone and is determined by Eq. 16. In the case of counter diffusion, Eq. 16 can be rewritten as:

$$U_r^1 = U_{r/V_2O_5}^1 + U_{r/MoO_3}^1 \qquad (31)$$

where $U_{r/V_2O_5}^1$ and U_{r/MoO_3}^1 are parts of the total U_r^1 generated at V_2O_5 and MoO_3 briquettes, respectively. It is easy to see that $U_{r/V_2O_5}^1$ should be zero, because electronic conductivity dominates in the α- and β-phases. On the other hand, U_{r/MoO_3}^1 may differ from zero, because it is produced at the product with the ionic (or mixed ionic-electronic) type of conductivity. So, in our case all parts of U_r^1 should be due to $^{V_2O_5}/MoO_3$ composite formation. If U_{r/MoO_3}^1 is not zero, it should be constant throughout the reaction and should vanish only after this process ends. However, a discrepancy arises: it was observed visually that the product layer did not occupy the whole MoO_3 briquette even after U_r decreased to 1–3 mV. Does this mean that the reaction product is localized outside the observable $^{V_2O_5}/MoO_3$ layer?

However, the very attempt to describe the U_r self-generation in cell 4 by Eq. 16 should be strongly criticized. Since both MoO_3 and $^{V_2O_5}/MoO_3$ possess considerable ionic conductivity (not less than 65% for MoO_3 and 55% for $^{V_2O_5}/MoO_3$ [4]), which is probably due to O^{2-}, Eqs. 17 and 18 are fulfilled. As a result, U_r in cell 4 approaches zero, which contradicts the experimental data. Thus, U_r self-generation in cell 4 cannot be explained by the interface reaction followed by a trivial separation of the space charge.

Secondly, the difference U_r is determined by the second term in Eq. 15, i.e. by Eq. 20. This model also predicts U_r^2 self-generation at the product with the ionic

(or ionic-electronic) type of conductivity, i.e. in this case U_r^2 is defined by U_{r/MoO_3}^2. The following situation is possible: a_{O2} at the $\beta|^{V_2O_5}/MoO_3$ boundary is defined by the ratio $[V^{5+}]/[V^{4+}]$ and a_{O2} at MoO_3 is equal to its counterpart in the surrounding gaseous atmosphere (air). Taking into account the high porosity of the substrate and the product (product porosity depends on the substrate porosity [2]) and considering the common gaseous phase, U_r^2 should be insignificant.

However, the main contradiction is connected with the inequality:

$$a_{O_2}\left(^{V_2O_5}/MoO_3|MoO_3\right) = 0.21 \gg a_{O_2}\left(\beta|^{V_2O_5}/MoO_3\right) \qquad (32)$$

leading to the polarity $(-)V_2O_5|MoO_3(+)$, opposite to the one observed in the experiment. So, neither of the above explanations is valid for U_r self-generation in cell 4.

Thirdly, let us consider the last term in Eqs. 14 and 15:

$$U_r^3 = U_{flow} \qquad (33)$$

Considering the properties of V_2O_5 and MoO_3 and the fact that U_r generation in cell 7 cannot be explained in terms of the theory of reaction potential difference, the term U_r^3 might be of special significance for the system at hand. In this case, mutual spreading of V_2O_5 and MoO_3 takes place owing to a relatively low specific surface energy and high surface diffusibility of both oxides.

It follows from Eq. 23 [14] that the vanadia flux should be much greater than the molybdena flux. Our findings contradict this conclusion, because the dominant reaction flux in the system under study is the molybdena one, which is in agreement with other results [4]. In our opinion, the tendency towards solid state spreading should not be treated by considering the diffusant crystalline structure only, without due regard to the substrate structure. Experimental results reported in this work suggest that this approach to solid state spreading is inadequate.

Let us return to Eq. 33. Analogously to Eq. 31, it may be rewritten as:

$$U_{flow} = U_r^3 = U_{r/V_2O_5}^3 + U_{r/MoO_3}^3 \qquad (34)$$

Consider each term in this relation. The first refers to generation of the potential difference when MoO_3 spreads over the electronic-conductivity ceramic V_2O_5. The second term characterizes the spreading of V_2O_5 over the surface of MoO_3, which is a mixed ionic-electronic conductor. Obviously, high electronic conductivity of V_2O_5 and the α,β-phases may lead to short-circuiting in the former case. As a result, U_r should be close to zero. The experimental value of U_r is negligible indeed (maximum 1 mV). Thus it may be assumed that the total U_r in cell 4 is determined by processes at the MoO_3 briquette only.

It is worth commenting on the composition of the complex transport form of vanadia. Let us take a closer look at the cells 11, 12, 13. Note that the vanadia source in cells 11 and 13 is $V_9Mo_6O_{40}$. Thus, the transport form should contain both vanadium and molybdenum atoms, since V_2O_5, MoO_3, and all intermediate phases (α, β, and $^{V_2O_5}/MoO_3$) have similar structures. In accordance with [10], the V_2MoO_8 β-phase consists of $[VO_6]$ and $[MoO_6]$ octahedra similar to polyhedra in the initial oxides V_2O_5 and MoO_3. They differ by the number ratios of octahedra that share vertices and edges. Thus molybdenum has no structural restrictions for participation in the vanadia transport form. It is noteworthy that such a process can change both the mobility and the spreading rate of vanadia.

As was mentioned in the foregoing, U_r self-generated in cell 4 had several specific features:

1. A large value compared to reactions with MoO_3 studied earlier [3].
2. The time dependence of U_r has two regions: a nearly constant (or slightly decreasing) U_r and a sharply decreasing U_r.
3. The length of first region depends on the initial thickness of the molybdena briquette. It should be noted that this fact was neglected in an earlier paper [3].

These experimental results disagree with Eq. 14. Probably they are due to vanadia spreading on the inner surface of the molybdena briquette, which may be viewed as a porous material with capillaries throughout. This proposition requires a theoretical substantiation.

However, the following model seems to be more realistic. The boundary interaction at the MoO_3 surface includes several stages. Firstly, V_2O_5 (or V-Mo-O) spreads over the surface of MoO_3, but vanadia cannot penetrate into the bulk of MoO_3 grains. Then molybdena out-diffuses through the vanadia film and forms the $^{V_2O_5}/MoO_3$ phase. This sequence correlates with a low surface energy of MoO_3. The U_r signal is generated owing to the mutual movement of MoO_3- and V_2O_5-enriched layers. This mechanism may fail to provide the V_2O_5 signal in the ESCA spectrum, which was measured some time after the sample was annealed.

In a later paper we shall try to explain the "strange" behavior of U_r with time and the molybdena briquette thickness, proceeding from the assumption of the vanadia spreading. Generation of U_r will be described in terms of the classical colloid theory of flow potential as applied to processes in cell 4.

Conclusion

The vanadia concentration of the product formed by vanadia transfer was determined using independent techniques: ESCA, CA, and NAA. It was found that a negligible vanadia quantity (minor reaction flux) was transferred into the molybdena briquette during a solid state reaction between V_2O_5 and MoO_3.

It was assumed that diffused vanadia was located in thin external layers of molybdena grains. However, the ESCA results showed that no vanadia was present on the molybdena grains. It was inferred that the most probable cause was the transfer of vanadia into molybdena grains upon cooling. The valence of the molybdenum atoms was found to be six.

The reaction potential difference in cell 4 was studied. It was found that:

1. The interaction between V_2O_5 and MoO_3 is accompanied by generation of a strong U_r signal.
2. U_r appears at the MoO_3 briquette and, consequently, is connected with the vanadia transport.
3. A more positive potential arises at the diffusant briquette (V_2O_5).

The time evolution of U_r has two regions. The potential U_r was constant (or diminished slightly) in the first region and decreased sharply in the second region. The length of the first region depended on the initial thickness of the MoO_3 briquette: the larger the thickness, the longer the period with nearly constant U_r.

The potential U_r was examined in cells 11, 12, 13, which present parts of cell 4. The total U_r due to the V_2O_5-MoO_3 interaction was produced in the formation and homogenization zone of the product on the MoO_3 surface, i.e. at the boundary between $^{V_2O_5}/MoO_3$ and MoO_3, which then moves into the depth of MoO_3.

U_r appears to be due to three different causes:

1. Chemical reaction.
2. Different a_{O2} values at the boundary between the reaction product and the initial oxides.
3. Spreading of the diffusant over the surface of the substrate: formation of a potential flow.

The last mechanism is most probable, but incomprehensible. It is connected with the fact that some oxides (MoO_3, V_2O_5, and WO_3) are capable of solid state spreading. Spreading is a phase process, which consists in the movement of large fragments of the crystal structure. It is known that a potential flow, which accompanies spreading, is formed in classic solid phase systems such as cells 11, 12, 13. The mechanism responsible for the reaction potential difference in cell 4 could not be due to (1) or (2). The reaction system at hand is similar to systems 11, 12, 13 and therefore the flow potential (3) could occur in cell 4. Mutual spreading of MoO_3 and V_2O_5 presents a specific feature of cell 4. In this case the transport form may have a mixed composition, including both molybdenum and vanadium atoms.

Finally, our experimental results may be explained in terms of the classic theory of potential flow.

392

References

1. Neiman AYa, Guseva AF (1993) Russ J Electrochem 29:1215
2. Neiman AYa, Guseva AF (1994) Kinet Catal 35:188
3. Neiman AYa, Guseva AF, Sharafutdinov AR (1997) Solid State Ionics 101–103:367
4. Neiman AYa (1996) Solid State Ionics 83:263
5. Neiman AYa, BarsanovSYu, Kharlov MV (1998) In: Ramanarayanan TA, Worrell WL, Tuller HL, Mogensen M, Khandkar AC (eds) Ionic and mixed conducting ceramics III. (ECS publications PV 97-24) The Electrochemical Society, Pennington, NJ, pp 219–228
6. Neiman AYa, Barsanov SYu (1999) Kinet Catal 40:50
7. Volkov VL, Tynkacheva GS, Fotiev AA, Tkachenko EV (1972) Russ J Inorg Chem 17:2803
8. Galahov F (ed) (1986) Diagramy sostoiania ogneupornih oxidov, vol 5, part 2. Nauka, Leningrad (in Russian)
9. Walczak J, Kurzawa M, Tabero P (1987) Thermochim Acta 118:1
10. Poray-Koshits MA, Atovmian LO (1974) Kristallohimmia i Stereohimiia Kordinatsionnih soedinenii Molibdena. Nauka, Moscow (in Russian)
11. Fotiev AA, Slobodin BV (1988) Vanadaty: sostav, struktura i svoistva. Nauka, Moscow (in Russian)
12. Kulikov IS (1986) Thermodinamika oxidov. Metallurgy, Moscow (in Russian)
13. Pavlov YuA (1974) Izvest Vyssh Uchebn Zaverd Chern Metall 14:25 (in Russian)
14. Leyrer J, Margraf R, Taglauer E, Knozinger H (1988) Surf Sci 201:603
15. Haber J (1984) Pure Appl Chem 56:1663
16. Haber J, Machej T, Grabowski R (1989) Solid State Ionics 32/33:887
17. Neiman AYa, Guseva AF (1999) Kinet Catal 40:38
18. NeimanA, Konisheva E (1998) Solid State Ionics 110:121
19. Rieger PhH (1994) Electrochemistry, 2nd edn. Chapman & Hall, New York
20. Neiman AYa, Utiumov V (1999) Solid State Ionics 119:43